

# Continuous Electricity Generation at High Voltages and Currents Using Stacked Microbial Fuel Cells

PETER AELTERMAN, KORNEEL RABAEY, HAI THE PHAM, NICO BOON, AND WILLY VERSTRAETE\*

Laboratory of Microbial Ecology and Technology (LabMET), Ghent University, Coupure Links 653, B-9000 Ghent, Belgium

Connecting several microbial fuel cell (MFC) units in series or parallel can increase voltage and current; the effect on the microbial electricity generation was as yet unknown. Six individual continuous MFC units in a stacked configuration produced a maximum hourly averaged power output of  $258 \text{ W m}^{-3}$  using a hexacyanoferrate cathode. The connection of the 6 MFC units in series and parallel enabled an increase of the voltages ( $2.02 \text{ V}$  at  $228 \text{ W m}^{-3}$ ) and the currents ( $255 \text{ mA}$  at  $248 \text{ W m}^{-3}$ ), while retaining high power outputs. During the connection in series, the individual MFC voltages diverged due to microbial limitations at increasing currents. With time, the initial microbial community decreased in diversity and Gram-positive species became dominant. The shift of the microbial community accompanied a tripling of the short time power output of the individual MFCs from  $73 \text{ W m}^{-3}$  to  $275 \text{ W m}^{-3}$ , a decrease of the mass transfer limitations and a lowering of the MFC internal resistance from  $6.5 \pm 1.0$  to  $3.9 \pm 0.5 \Omega$ . This study demonstrates a clear relation between the electrochemical performance and the microbial composition of MFCs and further substantiates the potential to generate useful energy by means of MFCs.

## Introduction

Microbial fuel cells (MFCs) convert chemical energy to electrical energy with the aid of microorganisms as biocatalysts (1). While being a marginal scientific issue for years, they have, in recent years, been catching up with other bioconversion concepts. New designs have evolved and the operation has been switched from fed-batch to continuous mode. (2, 3). Many authors have attempted to increase the MFC power output by the isolation of specific microbial organisms (4), by selecting for mediator producing organisms (5, 6), or by electrochemical optimization of the electrode surface (7).

MFC voltages will remain limited; even neglecting the internal losses, the voltage will never exceed a theoretical open circuit voltage (OCV) of  $1.14 \text{ V}$  as determined by the NADH ( $-0.32 \text{ V}$ ) and pure oxygen ( $+0.82 \text{ V}$ ) redox potentials (8). The highest OCV thus far reported of  $0.80 \text{ V}$  (9) illustrates this limitation. The maximum current on the other hand is determined by the (i) MFC design which determines the electrochemical losses (e.g., internal resistance) and convective transport limitations (5, 10), (ii) the volumetric loading which represents the total amount of electrons delivered by

the substrate for current production, and finally, (iii) the amount of substrate converted to electricity (the Coulombic efficiency).

The use of series or parallel stacked MFCs are essential to increase the voltages and currents produced by MFCs. Connecting several fuel cells in series adds the voltages, while one common current flows through all fuel cells (11). In case several power sources are connected in parallel, the voltage averages and the currents are added. Any desired current or voltage could be obtained by combining the appropriate number of series and parallel connected fuel cells or power sources. However, electricity production in a MFC is a microbial process and compliant to external conditions (10, 12). Hence, the external circuit could have an effect on the microbial electricity production. Furthermore, the MFC units in a series or parallel connection might not work independently and might be influenced by the electricity production of other MFCs. Up till now, the effect of the series and parallel connection on the microbial catalyst activity in a MFC stack is not known.

In a MFC, the microorganisms are structured in a biofilm and live in close contact with the electrode (4). An adaptation or change of the microbial community will influence the biofilm structure and its properties (13). The biofilm is part of the electrolyte; hence, alterations of the composition or structure of the biofilm might influence the electrochemical characteristics and losses of the MFC. In a MFC the electrochemical losses are categorized as (i) activation losses which can be lowered by the microbial production of electron shuttle or nanowires (5, 6, 14), (ii) ohmic losses which are determined by the resistance of the electrolyte and electrodes, and (iii) mass transfer losses which occur due to a decrease of reactants on the electrode surface (11, 15). Thus far, a relation between the electrochemical parameters on one hand and the evolution of the microbial community on the other hand has not been established.

In this research, a stacked MFC consisting of six identical MFCs was used to (i) investigate the influence of the electrical circuit (series or parallel) on the power, voltage and current output of the overall stack and the MFC units in the stack and (ii) to monitor the evolution between the microbial community and electrochemical characteristic of the individual MFCs.

## Material and Methods

**Microbial Fuel Cell Stack.** The MFC stack consisted of six individual MFC units (Figure 1). They were constructed of 12 identical Perspex frames. In the frames, both a sample port and two inlets were constructed and 2 partitions were installed to obtain a complete flow through. A robust cation exchange membrane (Ultrex CMI7000, Membranes International Inc., U.S.) was used between the anode and cathode of each MFC unit. The six MFCs were separated by five rubber sheets. Both the anode and cathode electrodes consisted of graphite granules to collect the electrons (type00514, diameter between 1.5 and 5 mm, Le Carbone, Belgium) and a graphite rod (5 mm diameter, Morgan, Belgium) to connect to the external circuit. Prior to use, the granules were washed three times with water. The separated MFCs in the stack were electrically connected in series or parallel using copper wires connected to the electrodes. The total empty volume of one frame was 156 mL. After installation of 2 partitions and the graphite electrode, the void volume of one frame amounted to 60 mL. This volume was used in the calculations.

**Operational Conditions.** The MFCs were operated at a room temperature of  $22 \pm 3 \text{ }^{\circ}\text{C}$ . A sterile synthetic influent

\* Corresponding author phone: +32 (0)9 264 59 76; fax: +32 (0)9 264 62 48; e-mail: Willy.Verstraete@UGent.be.

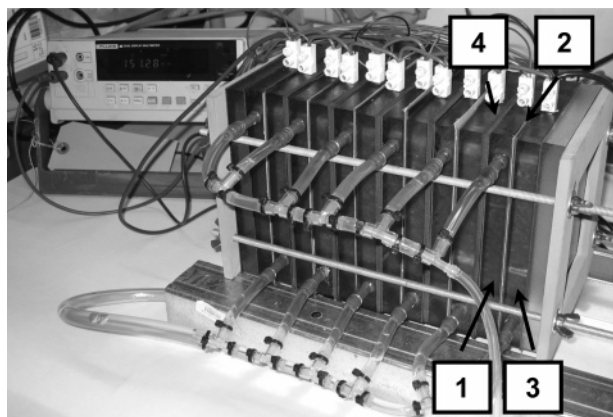


**FIGURE 1. Parallel connected stack microbial fuel cell (MFC) consisting of six individual microbial fuel cells (MFCs) with (1) a granular graphite anode, (2) an Ultrex cation exchange membrane, and (3) a 50 mM hexacyanoferrate cathode separated by (4) a rubber sheet.**

containing 0.75 to 1.00 g L<sup>-1</sup> sodium acetate (0.58–0.78 g chemical oxygen demand (COD) L<sup>-1</sup>) prepared as previously described (16) was continuously fed to the individual MFC anodes by a peristaltic pump (Watson Marlow, Belgium) at a flow rate of 7–21.1 mL h<sup>-1</sup> corresponding to a hydraulic retention time (HRT) of 8.86–2.86 h. Each MFC had a recirculation loop with a flow rate of 106 mL h<sup>-1</sup>. Unless stated otherwise, at day 104 a volumetric loading rate of 1.62 g COD L<sup>-1</sup> d<sup>-1</sup> was provided; 70 days later the volumetric loading rate was increased to 2.17 g COD L<sup>-1</sup> d<sup>-1</sup>.

The catholyte was prepared according to Park and Zeikus (7) and consisted of 50 mM K<sub>3</sub>Fe(CN)<sub>6</sub> aqueous solution in a 100 mM KH<sub>2</sub>PO<sub>4</sub> buffer (Merck, Belgium) adjusted to pH 7 with 1 M NaOH. The catholyte was recirculated through the cathodic matrix. The oxidation/reduction potential of the catholyte was controlled by either (i) a periodic renewal of the catholyte solution upon decolorization or (ii) a continuous electrochemical regeneration of the catholyte in an electrolysis cell.

**Inoculation, Start-Up, and Experimental Timing.** The anodic compartments of the MFC stack were inoculated with a mixture of anaerobic (Dendermonde, Belgium) and aerobic (Gent, Belgium) sludge. During start-up (day 0 to day 103), the stack was operated on several wastewaters: a domestic wastewater collected from a hospital (Ghent, Belgium) and two industrial organic streams: the influent and effluent of an anaerobic digester from a potato processing factory (Waregem, Belgium). Different operational conditions were imposed. Due to the qualitative variability of the influent and the limitations this represented regarding data processing and interpretation, the experiments were continued using a synthetic influent. This allowed us to increase the reproducibility. Three MFC duplicates with a common recirculation buffer vessel were installed at day 104. Starting from day 132, several analyses were conducted. The electrochemical analyses were made at regular intervals of approximately one month and were classified in three periods in time starting from the date of inoculation. The three periods in time are termed time 1 from day 132 to day 167, time 2 at day 175, and time 3 from day 200 to day 204.

**Calculations of the Electrical Parameters.** The electrodes were connected in series, parallel, or individual over an external resistance (*R*) (from 1.5 to 6000 Ω). The potential (*V*) of the six individual MFCs and the Coulombic efficiency was measured according to (2).

To calculate power density, a void volume of 60 mL (individual MFC) or 360 mL (stacked MFC) was used. The short time power densities were calculated using the instant

values obtained from the polarization curves. The hourly averaged power densities were calculated using the moving average of 60 voltage measurements during 1 h.

**Electrochemical Analysis.** The internal resistance was determined using the current interrupt method (11, 15). When the MFC produced a stable current output (*I*) and potential (*V*), the circuit was opened causing an initial steep potential (*V<sub>R</sub>*) rise followed by a further slow increase of the potential (*V<sub>A</sub>*). The steep increase is referred to as the ohmic losses caused by the internal resistance (*R<sub>int</sub>*). *R<sub>int</sub>* can thus be calculated as

$$R_{\text{int}} = V_R / I \quad (4)$$

The anode potential was measured using an Ag/AgCl (197 mV versus SHE) reference electrode (BASi, Warwickshire, United Kingdom).

Polarization curves were obtained by imposing a linear potential decrease followed by a linear voltage increase while measuring the current using a Bi-Stat potentiostat (Princeton Applied Research, Claix, France). The scan rate was 1 mV sec<sup>-1</sup>.

**Microbial Community Analysis.** Using a 10 mL syringe with a 0.9 × 90 mm spinal needle (BD Needles, Erembodegem, Belgium) biomass was scraped off the anode granules and subsequently sampled. Total DNA extraction (17) and 16S rRNA analysis for all Bacteria and PCR-DGGE analysis was done as described previously (6, 18).

Nucleotide sequences for bands 1–8 and bands A–C have been deposited in GenBank database under accession number DQ315499–DQ315509. More information can be found on page S2 of the Supporting Information.

## Results

**Stacked MFCs Provided Power at Enhanced Voltage and Current.** To increase the overall stack voltage or current, the six individual MFCs (called MFC 1 to MFC 6) were respectively connected in series or parallel. This resulted in an open circuit voltage (OCV) of 0.67 V for the parallel connection and 4.16 V for the series connection. The series stack produced a short circuit current (SCC) of 84.7 mA while the parallel stack delivered a SCC of 425.0 mA. Both OCV and SCC were approximately a factor of 6 higher than OCVs or SCC of the individual MFCs (Table 1). The short time power output of the series and parallel stack assessed at time 1 were similar and equalled 107 W m<sup>-3</sup>. At time 3, approximately 54 days later, the maximum short time power densities had almost tripled to 308 W m<sup>-3</sup> (series) and 263 W m<sup>-3</sup> (parallel) (Figure 2). The maximum short time power output of the series and parallel stack were of the same order of magnitude. However, the series stack produced this power at a higher voltage of 2279 mV (49 mA), while the parallel stack delivered an increased current of 269 mA at 354 mV (Figure 2). Based upon the polarization curves, the optimal external resistance was 49.1 Ω (series) and 1.3 Ω (parallel) at time 3 (Table 1). Using the optimal resistances, the hourly averaged maximum power outputs of the series and parallel stack were assessed and amounted to respectively 228 W m<sup>-3</sup> (at 2.02 V and 41.0 mA) and 248 W m<sup>-3</sup> (at 0.35 V and 255 mA). The Coulombic efficiency was 12.4%, for the series connection and 77.8% for the parallel connection, both based on a volumetric loading of 5.6 kg COD m<sup>-3</sup> d<sup>-1</sup>. The high power outputs obtained during short time polarization experiments could be maintained for at least 1 h under stacked conditions i.e., at enhanced voltage or current.

**Individual MFC Voltages Influenced by Series Connection at Higher Currents.** At time 1 the series circuit was closed using a variable external resistance (6000–15 Ω). The individual MFCs voltages and the overall stack voltage were monitored at several currents during 30 min periods (Figure

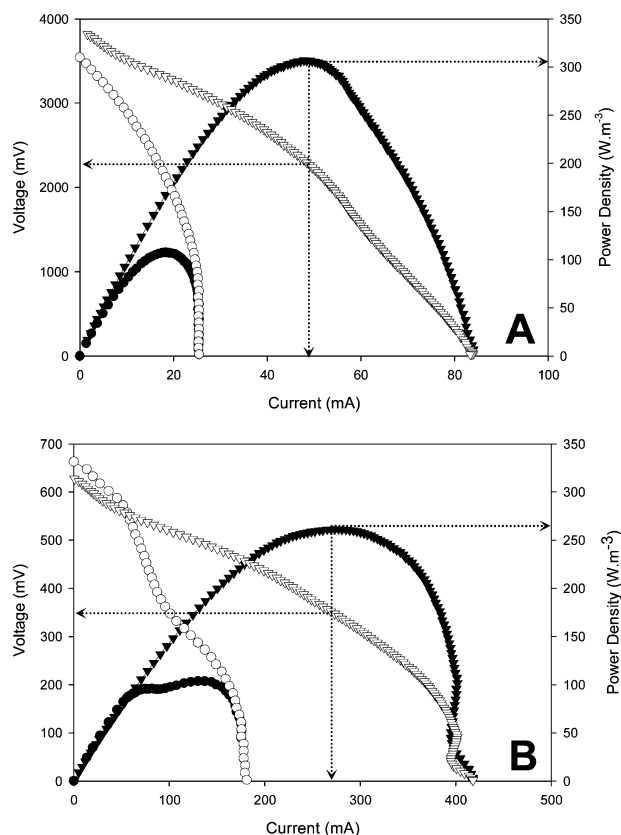


**FIGURE 2. Polarization curve (white) and power density-current curve (black) at time 1 (circle) and time 3 (triangle) of (A) the in series connected stack and (B) the in parallel connected stack both with a hexacyanoferrate cathode. The arrows indicate the voltage and current at the maximum short time power density.**

3). At external resistances of 6000–510  $\Omega$ , corresponding with low currents of 0.7–7.4 mA, low variances between the voltages of the individual MFCs were observed. However, starting from 360  $\Omega$  (10.1 mA) the individual MFC voltages started to diverge. This resulted in an unequal distribution of the individual MFCs voltages. The voltage differences between the MFCs increased to as much as 0.99 V. The latter was even accompanied with negative voltages or a reverse of polarity of three individual MFCs (MFC 3 to MFC 6). The voltages of MFC 4 to MFC 6 increased and returned to their normal state when the series stack was separated in individual MFCs. Despite the increasing variance between the MFC voltages, the total stack voltage followed a linear ohmic decrease with increasing current until 90  $\Omega$  (27.7 mA) when voltage dropped faster.

**Mutual and Time-Related Electrochemical Differences of the Individual MFCs.** Large differences between the performance of the stack MFC at time 1 and time 3 could be observed. In addition, differences in power output between the individual MFCs 1–6 were noticed. These significant differences were examined using basic electrochemical analysis, polarization curves, and a molecular analysis. Table 1 gives an overview of the electrochemical parameters of the individual MFCs and both the series and parallel stack. At time 1, the average internal resistance ( $R_{int}$ ) of the six MFCs was  $6.5 \pm 1.0 \Omega$ . Remarkably, at time 3 the average  $R_{int}$  was lowered to  $3.9 \pm 0.5 \Omega$ . In contrast to the  $R_{int}$ , the OCVs of the six MFCs were similar and averaged  $0.69 \pm 0.01$  V (time 1) and  $0.67 \pm 0.01$  V (time 3). The SCC produced by the six MFCs at time 1 showed large differences and were 2 times lower than currents at time 3 which were in addition very equal.

To further elucidate the evolution of the electrochemical response of the six MFCs, polarization curves were recorded at time 1, 2, and 3 (Figure 4). Three distinct polarization graphs were obtained for MFC 2, MFC 4, and MFC 6 (their respective duplicates MFC 1, 3, and 5 were analogous). At time 1, the voltage curves of MFC 4 and 6 decreased linearly. However, the voltage curve of MFC 2 showed a return at higher currents, despite its better performance (Figure 4). In addition, there was a notable difference in the maximum power density of MFC 6 ( $73 W m^{-3}$  at 12.2 mA) and of MFC 2 ( $167 W m^{-3}$  at 30.3 mA). At time 2, the power output of all MFCs had increased, resulting in maximum power densities of  $144 W m^{-3}$  at 25.8 mA (MFC 6) and  $200 W m^{-3}$  at 36.6 mA (MFC 2). Despite the overall increase, the voltage and power density curves of all the MFCs bended back starting at currents from 35 mA (MFC 6) to 40 mA (MFC 2), indicating limiting processes in all MFCs. At time 3, power output had further increased to levels of  $265 W m^{-3}$  at 49.0 mA (MFC 4) and  $281 W m^{-3}$  at 51.1 mA (MFC 2) and strikingly, no return of the voltage curves of the six MFCs could be observed. Moreover both shape and height of the symmetrical power density curves were very identical and power outputs reached high levels.

**Evolution of the Microbial Community in the Individual MFCs.** The Denaturing Gradient Gel Electrophoresis (DGGE) patterns of the individual MFCs at time 1 and 3 were used to monitor changes in the microbial community (Figure 5). Cluster analysis of the community at time 1, grouped the three MFC duplicates. The Pearson correlation for each duplicate was at least 80%. However, a low similarity between the three duplicates existed. The DGGE profile of the MFCs at time 3 revealed major shifts in the band pattern. Cluster analysis indicated a strong resemblance of the microbial composition between the six individual MFCs at time 3 (Pearson correlation over 97%). The microbial composition of time 3 and time 1 showed no correlation. To identify the most abundant ribotypes at time 1, bands were excised and sequenced. The major part of the identified species belonged to the phylum of the *Proteobacteria*. The other identified species were members of the *Firmicutes* and the *Actinobacteria*. For time 3, the 16S rRNA genes of one MFC were cloned and 40 clones were screened by DGGE. Clones representing bands A, B, and C accounted for, respectively, 13, 38, and 8% of all clones sequences (Figure 5). Sequencing showed that the mutual differences of the representative clones of the three bands were low (>98% similarity) and that all the clones were similar to *Brevibacillus agri* (99% similarity), belonging to the *Firmicutes*.

**Microbial Community and MFC Design Sustained High Performance.** The operation of the three best performing individual MFCs was evaluated in order (i) to compare with the stack performance and (ii) to assess long term power output. Using the averaged optimal external resistances for the individual MFCs at time 3 resulted in a maximum hourly averaged power density of  $189 \pm 6 W m^{-3}$  ( $n = 3$ ) ( $7.2 \Omega$ ) at a Coulombic efficiency of  $76.2 \pm 1.2\%$  ( $B_v = 6.6 g COD L^{-1} day^{-1}$ ). At an external resistance of 10  $\Omega$ , power output was higher and reached  $258 \pm 3 W m^{-3}$  ( $n = 3$ ) at a Coulombic efficiency of  $71.6 \pm 0.4\%$  or a substrate to electricity conversion of  $4.7 \pm 0.1 g COD L^{-1} d^{-1}$ . After 5 h, power had lowered to  $146 \pm 2 W m^{-3}$ , but remained roughly constant at this level for 11 more hours.

## Discussion

**The Stack Provided High Power Densities at Enhanced Voltages and Currents.** This paper demonstrates the use of stacked MFCs (both in series and parallel) to produce high power densities at enhanced voltages or currents. The maximum power outputs were unaffected by the series or



**TABLE 1. Internal Resistance ( $R_{int}$ ), Optimal External Resistance ( $R_{opt}$ ), Short Circuit Current (SCC), and Open Circuit Voltage (OCV) of the Average ( $n = 6$ ) of the Six Individual MFCs, the In-Series Connected Stack and the In Parallel Connected Stack, All Operating with a Hexacyanoferrate Cathode at Time 1 and Time 3<sup>a</sup>**

	time 1				time 3			
	$R_{int}$ ( $\Omega$ )	$R_{opt}$ ( $\Omega$ )	SCC (mA)	OCV (mV)	$R_{int}$ ( $\Omega$ )	$R_{opt}$ ( $\Omega$ )	SCC (mA)	OCV (mV)
average MFCs	$6.5 \pm 1.0$	$19.2 \pm 9.0$	$31.4 \pm 7.8$	$693 \pm 1$	$3.9 \pm 0.5$	$7.2 \pm 1.0$	$74.7 \pm 5.8$	$671 \pm 7$
series	nd <sup>b</sup>	113.7	25.5	4158	nd <sup>b</sup>	49.1	84.7	nd <sup>b</sup>
parallel	nd <sup>b</sup>	2.1	177.1	668	nd <sup>b</sup>	1.3	425.0	nd <sup>b</sup>

<sup>a</sup> The data of the 6 individual MFCs can be found in table S1 of the Supporting Information. <sup>b</sup> nd: not determined.

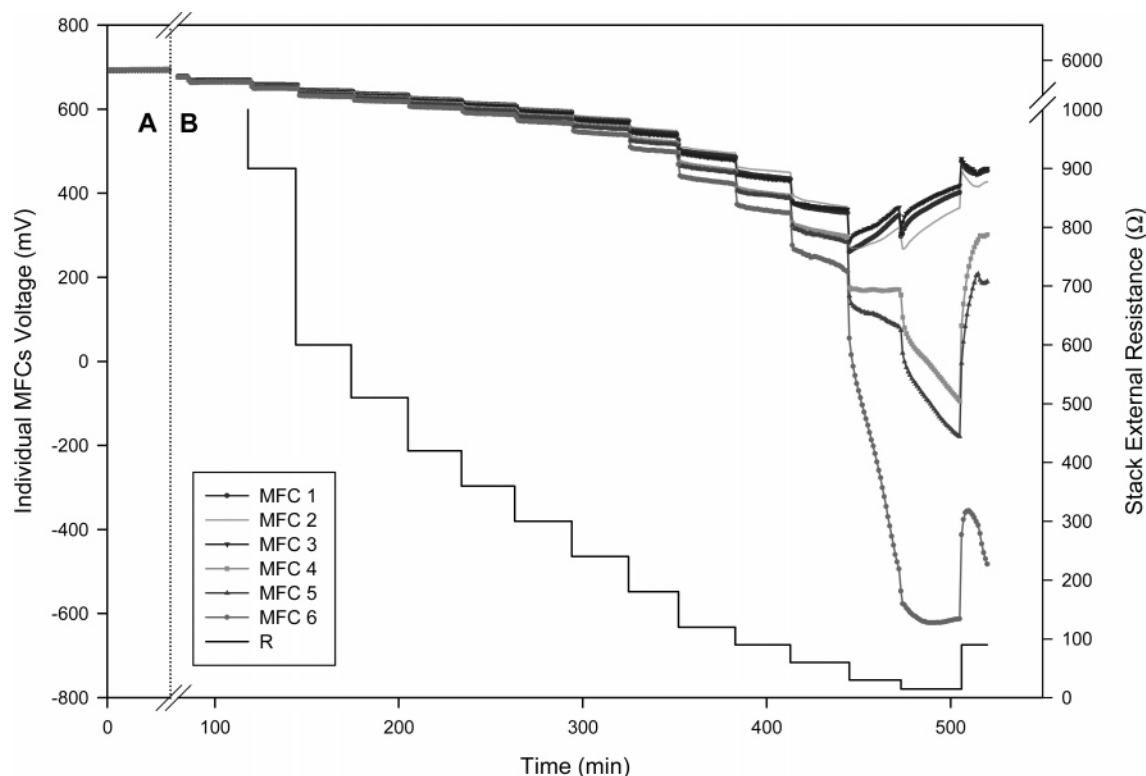


**FIGURE 3. Individual MFC voltages of the in series connected stack with a hexacyanoferrate cathode at (A) open circuit voltage (OCV) and (B) during a periodical (30 min) lowering of the stack external resistance ( $R$ ) from 6000 to 15  $\Omega$ . The total stack voltage is the sum of the six individual MFC voltages.**

parallel connection although individual MFCs could produce a higher hourly averaged power output. The reported hourly averaged power outputs were the highest thus far observed in continuous systems. They were almost three times higher compared to both the previous reported power densities for hexacyanoferrate and platinum coated cathode systems (2, 19). Despite the good cathodic performance of hexacyanoferrate, it is not regarded as sustainable.

A large difference between the Coulombic efficiency of the series and parallel connected stack was noted. Since both systems were operated at the same volumetric loading rate, this difference was caused by a 6 times lower current production of the series connection compared to the current production of the parallel connection. Thus, the connection of MFCs in series will not allow high current densities. However, if rapid COD removal and hence high current densities are required, the use of a individual MFCs or MFCs connected in parallel is appropriate.

By combining the individual polarization curves, one can deduce that the MFCs connected in series and parallel, worked, respectively, at an average current and voltage determined by the performance of the individual MFCs. As a consequence, stacked MFCs will not deliver higher power

densities than the individual MFCs. Yet, they create the possibility to produce an averaged power at more practical voltages and currents.

**During the series connection, large differences of the individual MFC voltages could be noted when currents increased.** Remarkably, the voltage of some MFCs in the stack even reversed polarity. This phenomenon is called cell reversal and also applies to proton exchange membrane fuel cells. Drawing excessive current from a fuel cell at a rate higher than its fuel delivery supports, leads to an increase of the anode potential and subsequent cell reversal. Fuel starvation, i.e., an inadequate supply of fuel, is a major cause of cell reversal and can occur during a sudden change of fuel demand such as during start-up or a change of the load (20). During our experiments, fuel delivery was adequate and the produced currents did not exceed the substrate loading rate. However, a rise of the anode potential (data not shown) and a subsequent cell reversal (Figure 3) could be observed. The MFCs which suffered cell reversal at time 1 produced a maximum current lower than the highest current during the series connection. This indicates that an excessive current might have been drawn from these MFCs during the series connection. The maximum current production is determined by

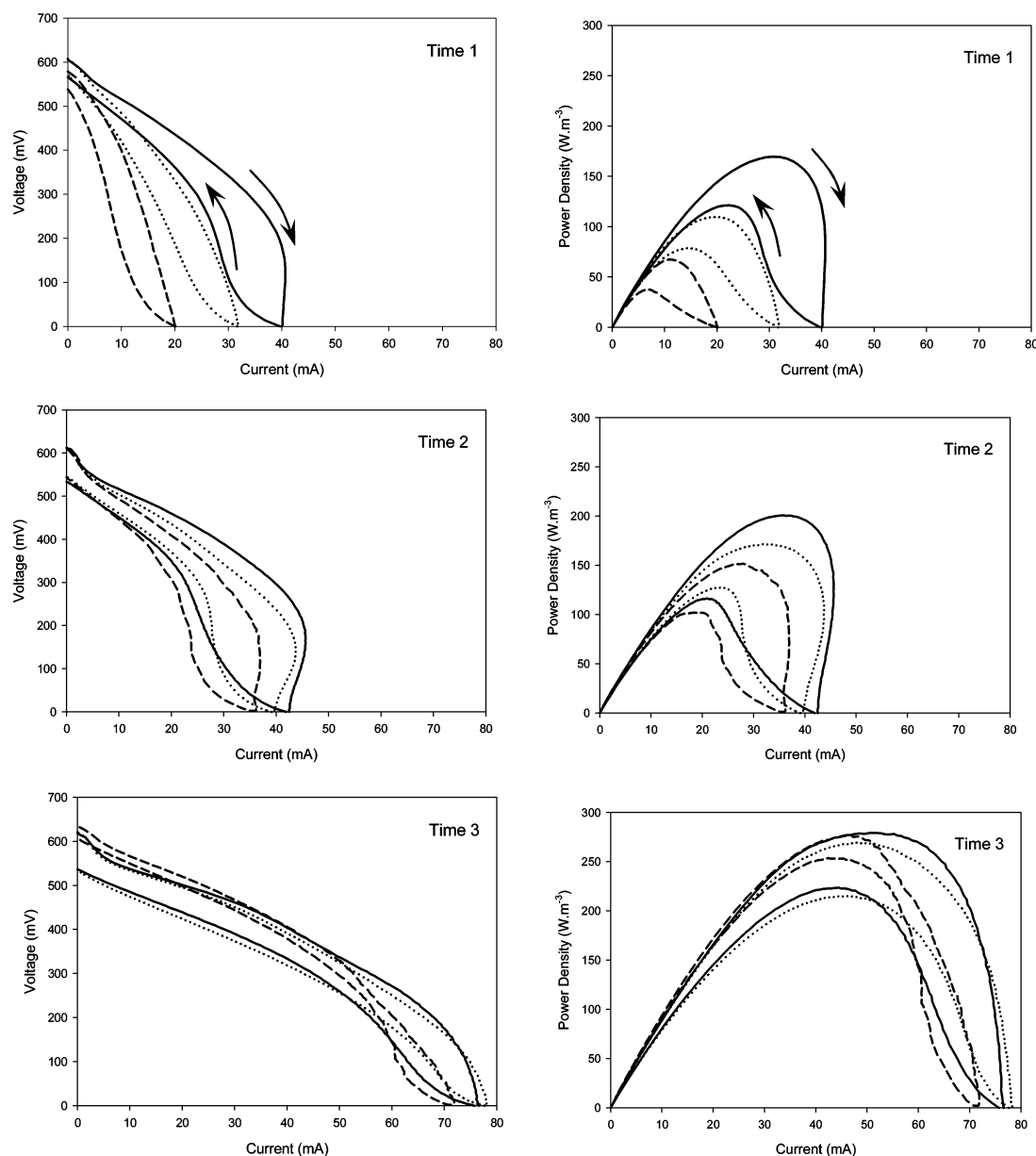


**FIGURE 4.** On and backward polarization curves of MFC 2 (solid line), MFC 4 (dotted line), and MFC 6 (dashed line) at time 1, time 2, and time 3 with the voltage (mV) as a function of the current (mA) (left). The curves on the right-hand describe the power density ( $\text{W m}^{-3}$ ) as a function of the current (mA). Polarization curves were recorded at a scan rate of  $1 \text{ mV sec}^{-1}$  and all MFCs used a hexacyanoferrate cathode.

the catalytic properties of the microbial consortium which influences both the rate and efficiency of the substrate to electric current conversion. Hence, since substrate delivery for all MFCs was adequate, the cell reversal was most likely a consequence of the limiting catalytic substrate conversion properties of some microbial consortia. This indicated that the external circuit had an influence on the microbial electricity production. However, a normal functioning of the MFCs was retrieved when disconnecting the stack to single MFCs.

**Gram-Positive Species Dominate Limited Anodophilic Consortium.** Major differences between the microbial community at time 1 and time 3 were observed. The microbial communities of the MFCs shifted from a mixed and diverse population to one very similar consortium for the distinguished MFCs, dominated by a limited amount of species. At time 1, most sequenced species were members of the *Proteobacteria*. All *Proteobacteria* are Gram-negative and are endowed with metabolic diversity (8). Several authors have

found members of the *Proteobacteria* in MFCs (21, 22). Some *Proteobacteria*, such as *Geobacter* (4) and *Shewanella* (23), have been successfully studied in MFCs. Our findings confirm these results and further substantiate the importance of the *Proteobacteria* as a pool for electricity producing bacteria.

Most strikingly, at time 3 when the performance was high, the microbial community was dominated by *Brevibacillus agri* a member of the Gram-positive *Bacilli* class. Two papers reported Gram-positive isolates respectively related to *Enterococcus gallinarum* (6) and *Clostridium butyricum* (24). At time 3, a previously described *Pseudomonas* species was also present but did not become dominant (6). However, the *Pseudomonas* species might have supported the electricity generation by producing mediators which are known to potentially enhance the electron transfer of other bacterial species (5). This finding urges the need to investigate the possible electron transfer differences between Gram-positive and Gram-negative species.

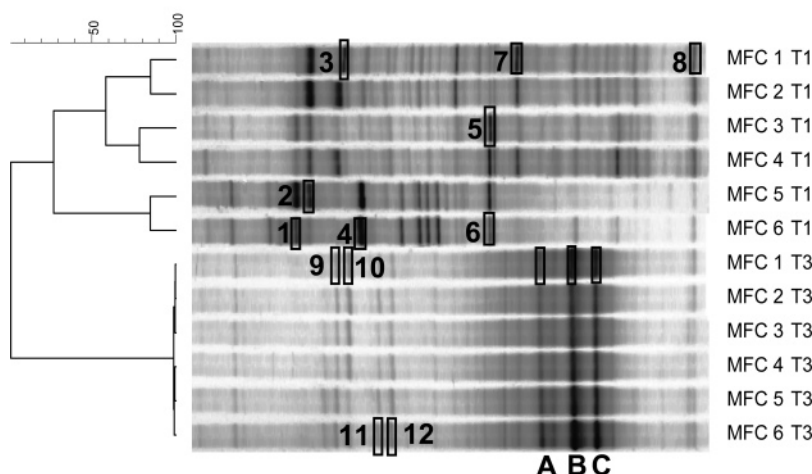


**FIGURE 5.** DGGE pattern of the microbial community of MFC 1 to MFC 6 at time 1 (T1) and time 3 (T3). The bands, which were cut out and sequenced, are numbered from 1 to 12. The bands representing a sequenced clone are numbered from A to C. The names of the organisms corresponding to the numbered bands can be found in table S2 of the Supporting Information.

**A Change of the Microbial Community Accompanied a Decrease of the Internal Resistance.** The current interrupt method, a straightforward but advantageous method to elucidate the internal resistance ( $R_{int}$ ) of the MFCs in the stack, indicated that the  $R_{int}$  values of the MFCs decreased over time. The measured  $R_{int}$  values were low compared to previous reports (25–29). As no modifications to the anode, cathode, or PEM had been made and the  $R_{int}$  decrease was independent of the increase of the acetate concentration in the medium; the  $R_{int}$  decrease was likely the result of an intrinsic alteration of the MFC microbial community itself. In MFCs the microorganisms grow as biofilms on the electrodes (4). Moreover, the microbial community determines the properties of the biofilm and its features (13). As a result, the adaptation or change of the microbial community might have an influence on the biofilm structure and properties. The latter also includes its electrochemical properties such as electrical conductivity and the presence of redox shuttles or nano-tubes (5, 6, 14, 30). Since the biofilm and the microbial community are part of the electrolyte they can influence the  $R_{int}$  of the MFC. This can indicate that the microbial community or its biofilm features may influence the electrochemical properties of the MFC resulting in a decrease of the  $R_{int}$ .

**Evolution of the Polarization Curves of the Individual MFCs.** Polarization curves provide several insights. The height of the polarization curves is related to overall performance of the MFC while the shape is related to the presence of the different polarizations or losses (11, 15). Starting at low currents, activation polarization can be discerned which is characterized by a steep initial drop of the potential. Next, the ohmic behavior of the electrolyte is reflected in a linear voltage drop at increasing currents. Finally, concentration or mass transfer losses are related to mass transfer limitations of both the influx of substrate and the removal of waste products and result in a rapid fall of the voltage at high currents. Our observations suggest, for the first time, the presence of mass transfer limitations in a MFC as deduced from the steep voltage drop and the return of the voltage curve at high currents (Figure 4). Even though an increase of the convection at time 1 should counter mass transfer issues, they could still be observed after increasing the recirculation rate (data not shown). This would indicate that the mass transfer losses occurred mainly within the biofilm.

However, at time 3, none of the MFCs showed a return of the voltage curve at high currents which is remarkable because, meanwhile, the maximum current had tripled. The evolution of the microbial community and the lowering of the internal resistance might explain the lower voltage drop at higher currents at time 3. The adaptation of the existing microbial community could have resulted in an optimal biofilm structure, which enabled a rapid uptake of substrate, a sufficient cycling of electron shuttles, and a rapid removal of protons and waste products. However, due to the complexity of this observation, more research is needed to unravel the precise mechanism.

**A Microbial and Electrochemical Relation.** This is the first report that relates the evolution of the electrochemical and microbial features of MFCs. Indeed, the shift from six different microbial communities to one limited consortium accompanied a decrease of the  $R_{int}$ , a shift in the polarization curves, and an overall increase of the power output. These findings favor the use of electrochemical techniques to elucidate the performance of both the microbial fuel cell design and the microbial community.

**Practical Implications and Future Research.** The good performance of stacked MFCs is a promising finding since for practical implementation high voltages and currents are required. However, if more MFCs are connected or higher current densities are achieved, the use of bipolar plates will be needed. Bipolar plates are placed between the anode and cathode of two adjacent MFCs and provide electrical conduction and mass separation (11). In this research, bipolar plates have been omitted to preserve maximum flexibility to change the external electrical connection. Furthermore, there is a need for cost-effective and robust cathodes. These major issues need to be dealt with in future designs but nevertheless the presented data underline the energy recovery potential of the MFC.

## Acknowledgments

This research was funded by a Ph.D grant (IWT grant no 41294) of the Institute for the Promotion of Innovation through Science and Technology in Flanders (IWT-Vlaanderen) and a fund of the Research Foundation—Flanders (FWO project G.0172.05). We thank Petra Vandamme for her help with the molecular analyses. The useful comments of Tom Defoirdt were highly appreciated.

## Supporting Information Available

The basic electrochemical characteristic of the individual MFCs, the procedure for the microbial community analysis, and the composition of the microbial community. This material is available free of charge via the Internet at <http://pubs.acs.org>.

## Literature Cited

- (1) Allen, R. M.; Bennetto, H. P. Microbial fuel-cells—electricity production from carbohydrates. *Appl. Biochem. Biotechnol.* **1993**, *39*, 27–40.
- (2) Rabaey, K.; Clauwaert, P.; Aelterman, P.; Verstraete, W. Tubular microbial fuel cells for efficient electricity generation. *Environ. Sci. Technol.* **2005**, *39*, 8077.
- (3) Liu, H.; Ramnarayanan, R.; Logan, B. E. Production of electricity during wastewater treatment using a single chamber microbial fuel cell. *Environ. Sci. Technol.* **2004**, *38*, 2281–2285.
- (4) Bond, D. R.; Lovley, D. R. Electricity production by *Geobacter sulfurreducens* attached to electrodes. *Appl. Environ. Microbiol.* **2003**, *69*, 1548–1555.
- (5) Rabaey, K.; Boon, N.; Höfte, M.; Verstraete, W. Microbial phenazine production enhances electron transfer in biofuel cells. *Environ. Sci. Technol.* **2005**, *39*, 3401–3408.
- (6) Rabaey, K.; Boon, N.; Siciliano, S. D.; Verhaege, M.; Verstraete, W. Biofuel cells select for microbial consortia that self-mediate electron transfer. *Appl. Environ. Microbiol.* **2004**, *70*, 5373–5382.
- (7) Park, D. H.; Zeikus, J. G. Improved fuel cell and electrode designs for producing electricity from microbial degradation. *Biotechnol. Bioeng.* **2003**, *81*, 348–355.
- (8) Madigan, M. T.; Martinko, J. M.; Parker, J. *Brock Biology of Microorganisms*; Prentice Hall: Upper Saddle River, NJ, 2000.
- (9) Liu, H.; Cheng, S. A.; Logan, B. E. Production of electricity from acetate or butyrate using a single-chamber microbial fuel cell. *Environ. Sci. Technol.* **2005**, *39*, 658–662.
- (10) Moon, H.; Chang, I. S.; Jang, J. K.; Kim, B. H. Residence time distribution in microbial fuel cell and its influence on COD removal with electricity generation. *Biochem. Eng. J.* **2005**, *27*, 59–65.
- (11) Larminie, J.; Dicks, A. *Fuel Cell Systems Explained*; John Wiley & Sons: Chichester, UK, 2000.
- (12) Liu, H.; Cheng, S. A.; Logan, B. E. Power generation in fed-batch microbial fuel cells as a function of ionic strength, temperature, and reactor configuration. *Environ. Sci. Technol.* **2005**, *39*, 5488–5493.
- (13) Sutherland, I. W. The biofilm matrix—an immobilized but dynamic microbial environment. *Trends Microbiol.* **2001**, *9*, 222–227.
- (14) Reguera, G.; McCarthy, K. D.; Mehta, T.; Nicoll, J. S.; Tuominen, M. T.; Lovley, D. R. Extracellular electron transfer via microbial nanowires. *Nature* **2005**, *435*, 1098–1101.
- (15) Hoogers, G. Fuel Cell Components and Their Impact on Performance. In *Fuel Cell Technology Handbook*; Hoogers, G., Ed.; CRC: Boca Raton, FL, 2003.
- (16) Rabaey, K.; Ossieur, W.; Verhaege, M.; Verstraete, W. Continuous microbial fuel cells convert carbohydrates to electricity. *Water Sci. Technol.* **2005**, *52*, 515–523.
- (17) Boon, N.; Goris, J.; De Vos, P.; Verstraete, W.; Top, E. M. Bioaugmentation of activated sludge by an indigenous 3-chloroaniline degrading *Comamonas testosteroni* strain, I2gfp. *Appl. Environ. Microbiol.* **2000**, *66*, 2906–2913.
- (18) Boon, N.; De Windt, W.; Verstraete, W.; Top, E. M. Evaluation of nested PCR-DGGE (denaturing gradient gel electrophoresis) with group-specific 16S rRNA primers for the analysis of bacterial communities from different wastewater treatment plants. *FEMS Microbiol. Ecol.* **2002**, *39*, 101–112.
- (19) Moon, H.; Chang, I. S.; Kim, B. H. Continuous electricity production from artificial wastewater using a mediator-less microbial fuel cell. *Bioresour. Technol.* **2006**, *97*, 621–627.
- (20) Taniguchi, A.; Akita, T.; Yasuda, K.; Miyazaki, Y. Analysis of electrocatalyst degradation in PEMFC caused by cell reversal during fuel starvation. *J. Power Sources* **2004**, *130*, 42–49.
- (21) Phung, N. T.; Lee, J.; Kang, K. H.; Chang, I. S.; Gadd, G. M.; Kim, B. H. Analysis of microbial diversity in oligotrophic microbial fuel cells using 16S rDNA sequences. *FEMS Microbiol. Lett.* **2004**, *233*, 77–82.
- (22) Kim, B. H.; Park, H. S.; Kim, H. J.; Kim, G. T.; Chang, I. S.; Lee, J.; Phung, N. T. Enrichment of microbial community generating electricity using a fuel-cell-type electrochemical cell. *Appl. Microbiol. Biotechnol.* **2004**, *63*, 672–681.
- (23) Kim, H. J.; Park, H. S.; Hyun, M. S.; Chang, I. S.; Kim, M.; Kim, B. H. A mediator-less microbial fuel cell using a metal reducing bacterium, *Shewanella putrefaciens*. *Enzyme Microb. Technol.* **2002**, *30*, 145–152.
- (24) Park, H. S.; Kim, B. H.; Kim, H. S.; Kim, H. J.; Kim, G. T.; Kim, M.; Chang, I. S.; Park, Y. K.; Chang, H. I. A novel electrochemically active and Fe(III)-reducing bacterium phylogenetically related to *Clostridium butyricum* isolated from a microbial fuel cell. *Anaerobe* **2001**, *7*, 297–306.
- (25) He, Z.; Minteer, S. D.; Angenent, L. T. Electricity generation from artificial wastewater using an upflow microbial fuel cell. *Environ. Sci. Technol.* **2005**, *39*, 5262–5267.
- (26) Jang, J. K.; Pham, T. H.; Chang, I. S.; Kang, K. H.; Moon, H.; Cho, K. S.; Kim, B. H. Construction and operation of a novel mediator- and membrane-less microbial fuel cell. *Process Biochem.* **2004**, *39*, 1007–1012.
- (27) Oh, S. E.; Min, B.; Logan, B. E. Cathode performance as a factor in electricity generation in microbial fuel cells. *Environ. Sci. Technol.* **2004**, *38*, 4900–4904.
- (28) Ieropoulos, I. A.; Greenman, J.; Melhuish, C.; Hart, J. Comparative study of three types of microbial fuel cell. *Enzyme Microb. Technol.* **2005**, *37*, 238–245.
- (29) Min, B.; Cheng, S.; Logan, B. E. Electricity generation using membrane and salt bridge microbial fuel cells. *Water Res.* **2005**, *39*, 1675–1686.
- (30) Bond, D. R.; Lovley, D. R. Evidence for involvement of an electron shuttle in electricity generation by *Geothrix fermentans*. *Appl. Environ. Microbiol.* **2005**, *71*, 2186–2189.

Received for review December 20, 2005. Revised manuscript received March 14, 2006. Accepted March 16, 2006.

ES0525511